Synthesis, Characterization, and Ethylene Oligomerization and Polymerization of Ferrous and Cobaltous 2-(Ethylcarboxylato)-6-iminopyridyl Complexes

Wen-Hua Sun,* Xiubo Tang, Tielong Gao, Biao Wu, Wenjuan Zhang, and Hongwei Ma

CAS Key Laboratory of Engineering Plastics, Institute of Chemistry, Chinese Academy of Sciences, Beijing 100080, China, and State Key Laboratory of Structural Chemistry, Fujian Institute of Research on the Structure of Matter, Chinese Academy of Sciences, Fuzhou 350002, China

Received May 12, 2004

A series of ferrous complexes (L)$FeCl_2$ (**3a**−**f**) and cobaltous complexes (L)$CoCl_2$ (**4a**−**f**) were prepared by the reaction of 2-(carboxylato)-6-iminopyridines **2a**−**f** (2-COOEt-6-(2,6-$R_2C_6H_3N{=}CCH_3$)C_5H_3N: **2a**, R = CH_3; **2b**, R = Et; **2c**, R = *i*-Pr; **2d**, R = F; **2e**, R = Cl; **2f**, R = Br) with $FeCl_2$ or $CoCl_2$. The obtained complexes were characterized by elemental analysis and IR spectroscopy, and the solid-state structures of **2b**,**c**, **3b**,**c**,**e**,**f**, and **4c**,**f** were determined by X-ray diffraction analysis. X-ray crystallographic analyses of complexes **3c**,**e**,**f** and **4c**,**f** reveal a four-coordinated distorted-tetrahedral geometry, except for complex **3b**, in which the tridentate ligand is coordinated through a weak bonding between iron and the carbonyl oxygen of the ester group. The complexes were studied for ethylene oligomerization and polymerization in the presence of methylaluminoxane (MAO) under various reaction conditions. It was found that the ferrous complexes exhibit higher activities for ethylene polymerization than for oligomerization, while the cobaltous complexes show higher activities for ethylene oligomerization. In addition, the ferrous catalytic systems predominantly produce linear oligomers and polyethylene with unsaturated end groups.

Introduction

Research interest in late-transition-metal complex catalysts for ethylene polymerization has undergone a phenomenal acceleration over the past decade.[1] The late-transition-metal complex catalysts have long been developed to produce dimers or low-molecular-weight oligomers by chain termination via β-hydride elimination.[2] As a milestone of late-transition-metal catalysts for ethylene polymerization, the discovery of diimine-based cationic catalysts[3] and 2,6-bis(imino)pyridyl-based cationic catalysts[4] resurrected the late-transition-metal complexes as the catalysts for ethylene polymerization and oligomerization by the SHOP process.[5] Recently, many academic and industrial research laboratories have engaged in exploring unknown organometallic precatalysts containing various philological [O−P],[6] [O−N],[7] [N−N],[8] [N−P],[9] and [N−N−N][10] ligands. Following the innovative finding of the highly active 2,6-bis(imino)pyridyl catalysts, numerous investigations have been conducted in search of the intermediates of catalytic systems,[11] in which the 2,6-bis(imino)pyridyl-based ferrous and cobaltous catalysts were modified by varying the substituent on the aryl group of the ligand.[12] Unfortunately, these efforts failed to generate active

* To whom correspondence should be addressed at the Chinese Academy of Sciences.

(1) (a) Britovsek, G. J. P.; Gibson, V. C.; Wass, D. F. *Angew. Chem., Int. Ed.* **1999**, *38*, 428−447. (b) Ittel, S. D.; Johnson, L. K.; Brookhart, M. *Chem. Rev.* **2000**, *100*, 1169−1203. (c) Gibson, V. C.; Spitzmesser, S. K. *Chem. Rev.* **2003**, *103*, 283−315.

(2) (a) Rix, F.; Brookhart, M. *J. Am. Chem. Soc.* **1995**, *117*, 1137−1138. (b) Peuckert, M.; Keim, W. *Organometallics* **1983**, *2*, 594−597. (c) Wilke, G. *Angew. Chem., Int. Ed. Engl.* **1988**, *27*, 185−206.

(3) (a) Johnson, L. K.; Killian, C. M.; Brookhart, M. *J. Am. Chem. Soc.* **1995**, *117*, 6414−6415. (b) Johnson, L. K.; Mecking, S.; Brookhart, M. *J. Am. Chem. Soc.* **1996**, *118*, 267−268. (c) Mecking, S.; Johnson, L. K.; Wang, L.; Brookhart, M. *J. Am. Chem. Soc.* **1998**, *120*, 888−899. (d) Killian, C. M.; Tempel, D. J.; Johnson, L. K.; Brookhart, M. *J. Am. Chem. Soc.* **1996**, *118*, 11664−11665. (e) Feldman, J.; McLain, S. J.; Parthasarathy, A.; Marshall, W. J.; Calabrese, J. C.; Arthur, S. D. *Organometallics* **1997**, *16*, 1514−1516.

(4) (a) Small, B. L.; Brookhart, M.; Bennett, A. M. A. *J. Am. Chem. Soc.* **1998**, *120*, 4049−4050. (b) Britovsek, G. P. J.; Gibson, V. C.; Kimberley, B. S.; Maddox, P. J.; McTavish, S. J.; Solan, G. A.; White, A. J. P.; Williams, D. J. *Chem. Commun.* **1998**, 849−850.

(5) (a) Keim, W.; Kowaldt, F. H.; Goddard, R.; Kruger, C. *Angew. Chem., Int. Ed. Engl.* **1978**, *17*, 466−467. (b) Keim, W. *Angew. Chem., Int. Ed. Engl.* **1990**, *29*, 235−244.

(6) (a) Komon, Z. J. A.; Bu, X.; Bazan, G. C. *J. Am. Chem. Soc.* **2000**, *122*, 1830−1831. (b) Komon, Z. J. A.; Bu, X.; Bazan, G. C. *J. Am. Chem. Soc.* **2000**, *122*, 12379−12380. (c) Kalamarides, H. A.; Iyer, S.; Lipian, J.; Rhodes, L. F.; Day, C. *Organometallics* **2000**, *19*, 3983−3990. (d) Malinoski, J. M.; Brookhart, M. *Organometallics* **2003**, *22*, 5324−5335.

(7) (a) Younkin, T. R.; Connor, E. F.; Henderson, J. I.; Friedrich, S. K.; Grubbs, R. H.; Bansleben, D. A. *Science* **2000**, *287*, 460−462. (b) Hicks, F. A.; Brookhart, M. *Organometallics* **2001**, *20*, 3217−3219. (c) Bauers, F. M.; Mecking, S. *Angew. Chem., Int. Ed.* **2001**, *40*, 3020−3022. (d) Shim, C. B.; Kim, Y. H.; Lee, B. Y.; Dong, Y.; Yun, H. *Organometallics* **2003**, *22*, 4272−4280. (e) Sun, W.-H.; Yang, H.; Li, Z.; Li, Y. *Organometallics* **2003**, *22*, 3678−3683. (f) Wang, L.; Sun, W.-H.; Han, L.; Li, Z.; Hu, Y.; He, C.; Yan, C. *J. Organomet. Chem.* **2002**, *650*, 59−64. (g) Sun, W.-H.; Zhang, W.; Gao, T.; Tang, X.; Chen, L.; Li, Y.; Jin, X. *J. Organomet. Chem.* **2004**, *689*, 917−929. (h) Chen, L.; Hou, J.; Sun, W.-H. *Appl. Catal. A* **2003**, *246*, 11−16. (i) Shim, C. B.; Kim, Y. H.; Lee, B. Y.; Dong, Y.; Yun, H. *Organometallics* **2003**, *22*, 4272−4280. (j) Hicks, F. A.; Jenkins, J. C.; Brookhart, M. *Organometallics* **2003**, *22*, 3533−3545.

10.1021/om0496636 CCC: $27.50
Publication on Web 09/10/2004

catalysts, and the catalytic activities of these ferrous and cobaltous complexes are disappointingly poor.[13] In the exploration of the scope of ferrous and cobaltous complex catalysts for ethylene polymerization, it has long been a goal to create ferrous catalysts which are as active as the bidentate chelated nickel analogues.[3,8] Indeed, the pyridylimine-based nickel and palladium[14] complexes serve as the active catalysts for ethylene polymerization, but the corresponding ferrous and cobaltous analogues do not show any activity. Clearly, to study iminopyridyl-based ferrous and cobaltous complexes for ethylene polymerization, a synthetic protocol for the preparation of the robust iminopyridyl ligands must be developed. We have established the procedure of synthesizing the ligands by preparing ethyl 6-acetylpyridine-2-carboxylate, which further reacts with arylamines to form 2-(carboxylato)-6-iminopyridine derivatives. We prepared a variety of 2-(carboxylato)-6-iminopyridine analogues with ortho-positioned alkyl and halogen substituents on the aryl rings and subsequently investigated the catalytic activities of their ferrous and cobatous complexes for ethylene oligomerization and polymerization. It was found that the asymmetric iminopyridyl ferrous and cobaltous complexes prepared, which are remarkably stable in air, exhibit high activities for ethylene polymerization and oligomerization. Our studies have provided an insight into the effects of the ligands on the ethylene oligomerization and polymerization behaviors of the complexes. In addition, the incorporation of the ester group into the ligand backbone has been found to affect the coordination environment around the metal center. We report herein the synthesis and characterization of 2-(carboxylato)-6-iminopyridine-based ferrous and cobaltous complexes and the investigation of their catalytic behaviors for ethylene oligomerization and polymerization upon activation with MAO.

Results and Discussion

1. Synthesis and Characterization of the Ligands and Complexes. Ethyl 6-acetylpyridine-2-carboxylate (**1**) was initially synthesized by the reaction of 2,6-dicarbethoxypyridine with ethyl acetate in the presence of C_2H_5ONa using the modified procedure for the synthesis of 2,6-diacetylpyridine.[15] The optimal molar ratio of C_2H_5ONa to 2,6-dicarbethoxypyridine was determined to be 1.1−1.5 in order to dominantly afford compound **1** in an acceptable yield, and with 2−5 equiv of C_2H_5Na, 2,6-diacetylpyridine was obtained as the major product. The pyridineimine ligands **2a**−**c** were easily prepared in satisfactory yields (68.2−73.0%) through the Schiff-base condensation of compound **1** with anilines in the presence of a catalytic amount of *p*-toluenesulfonic acid (*p*-TsOH) in refluxing toluene. To synthesize **2d**−**f**, which are halogen-substituted on the aryl ring, a small amount of silica−alumina catalyst support (grade 135) was added to the reaction mixtures in addition to the catalytic amount of *p*-TsOH.[12d,k] Moreover, the reactions were assisted by the addition of 4 Å molecular sieves as water absorbent (Scheme 1).

Ligands **2a**−**f** were characterized by IR spectra, ^{1}H NMR, ^{13}C NMR, and elemental analysis, and **2b**,**c** were further characterized by X-ray diffraction analysis (Figure 1). Both **2b** and **2c** are in the *E* conformation with typical imino C═N double bond lengths of 1.266(3) and 1.272 Å, respectively. For **2b** and **2c** in the solid state, the aryl rings on imine are approximately perpendicular to the pyridine rings, and their dihedral angles are 104.5 and 92.5°, respectively. The ethyl and ester groups on the ligand **2b** are flexible and disordered, due to their free rotation. Additionally, the X-ray diffraction determination reveals that there are two

(8) (a) Lee, B. Y.; Bazan, G. C.; Vela, J.; Komon, Z. J. A.; Bu, X. *J. Am. Chem. Soc.* **2001**, *123*, 5352−5353. (b) Domhover, B.; Klaui, W.; Kermer-Aach, A.; Bell, R.; Mootz, D. *Angew. Chem., Int. Ed.* **1998**, *37*, 3050−3052. (c) Li, J.; Gao, T.; Zhang, W.; Sun, W.-H. *Inorg. Chem. Commun.* **2003**, *6*, 1372−1374. (d) Diamanti, S. J.; Ghosh, P.; Shimizu, F.; Bazan, G. C. *Macromolecules* **2003**, *36*, 9731−9735. (e) Sun, W.-H.; Shao, C.; Chen, Y.; Hu, H.; Sheldon, R. A.; Wang, H., Leng, X.; Jin, X. *Organometallics* **2002**, *21*, 4350−4355. (f) Foley, S. R.; Stockland, R. A., Jr.; Shen, H.; Jordan, R. F. *J. Am. Chem. Soc.* **2003**, *125*, 4350−4361. (g) Salo, E. V.; Guan, Z. *Organometallics* **2003**, *22*, 5033−5046.

(9) (a) Chen, H.-P.; Liu, Y.-H.; Peng, S.-M.; Liu, S.-T. *Organometallics* **2003**, *22*, 4893−4899. (b) Speiser, F.; Braunstein, P.; Saussine, L.; Welter, R. *Inorg. Chem.* **2004**, *43*, 1649−1658. (c) Sun, W.-H.; Li, Z.; Hu, H.; Wu, B.; Yang, H.; Zhu, N.; Leng, X.; Wang, H. *New J. Chem.* **2002**, *26*, 1474−1478. (d) Shi, P.-Y.; Liu, Y.-H.; Peng, S.-M.; Liu, S.-T. *Organometallics* **2002**, *21*, 3203−3207. (e) Daugulis, O.; Brookhart, M. *Organometallics* **2002**, *21*, 5926−5934. (f) Daugulis, O.; Brookhart, M.; White, P. S. *Organometallics* **2002**, *21*, 5935−5943.

(10) (a) Britovsek, G. J. P.; Gibson, V. C.; Kimberley, B. S.; Mastroianni, S.; Redshaw, C.; Solan, G. A.; White, A. J. P.; Williams, D. J. *Dalton* **2001**, 1639−1644. (b) Michiue, K.; Jordan, R. F. *Organometallics* **2004**, *23*, 460−470. (c) Kunrath, F. A.; de Souza, R. F.; Casagrande, O. L., Jr.; Brooks, N. R.; Young, V. G., Jr. *Organometallics* **2003**, *22*, 4739−4743. (d) Wang, L.; Sun, W.-H.; Han, L.; Yang, H.; Hu, Y.; Jin, X. *J. Organomet. Chem.* **2002**, *658*, 62−70.

(11) (a) Gibson, V. C.; Humphries, M. J.; Tellmann, K. P.; Wass, D. F.; White, A. J. P.; Williams, D. J. *Chem. Commun.* **2001**, 2252−2253. (b) Ramos, J.; Cruz, V.; Munoz-Escalona, A.; Martinez-Salazar, J. *Polymer* **2003**, *43*, 3635−3645. (c) Britovsek, G. J. P.; Gibson, V. C.; Spitzmesser, S. K.; Tellmann, K. P.; White, A. J. P.; Williams, D. J. *Dalton* **2002**, 1159−1171. (d) Talsi, E. P.; Babushkin, D. E.; Semikolenova, N. V.; Zudin, V. N.; Panchenko, V. N.; Zakharov, V. A. *Macromol. Chem. Phys.* **2001**, *202*, 2046−2051. (e) Luo, H.; Yang, Z.-H.; Mao, B.-Q.; Yub, D.-S.; Tang, R.-G. *J. Mol. Catal. A* **2002**, *177*, 195−207. (f) Kooistra, T. M.; Knijnenburg, Q.; Smits, J. M. M.; Horton, A. D.; Budzelaar, P. H. M.; Gal, A. W. *Angew. Chem.* **2001**, *113*, 4855−4858.

(12) (a) Britovsek, G. J. P.; Bruce, M.; Gibson, V. C.; Kimberley, B. S.; Maddox, P. J.; Mastroianni, S.; McTavish, S. J.; Redshaw, C.; Solan, G. A.; Stro1mberg, S.; White, A. J. P.; Williams. D. J. *J. Am. Chem. Soc.* **1999**, *121*, 8728−8740. (b) Amort, C.; Malaun, M., Krajete, A.; Kopacka, H.; Wurst, K.; Christ, M.; Lilge, D.; Kristen, M. O.; Bildstein, B. *Appl. Organomet. Chem.* **2002**, *16*, 506−516. (c) Small, B. L.; Brookhart, M. *J. Am. Chem. Soc.* **1998**, *120*, 7143−7144. (d) Chen, Y. F.; Qian, C. T.; Sun, J. *Organometallics* **2003**, *22*, 1231−1236. (e) Paulino, I. S.; Schuchardt, U. *J. Mol. Catal. A* **2004**, *211*, 55−58. (f) Ma, Z.; Sun, W.-H.; Zhu, N.; Li, Z.; Shao, C.; Hu, Y. *Polym. Int.* **2002**, *51*, 349−352. (g) Abu-Surrah, A. S.; Lappalainen, K.; Piironen, U.; Lehmus, P.; Repo, T.; Leskela, M. *J. Organomet. Chem.* **2002**, *648*, 55−61. (h) Britovsek, G. J. P.; Mastroianni, S.; Solan, G. A.; Baugh, S. P. D.; Redshaw, C.; Gibson, V. C.; White, A. J. P.; Williams. D.; Elsegood, M. R. J. *Chem. Eur. J.* **2000**, *6*, 2221−2231. (i) Bluhm, M. E.; Folli, C.; Döring, M. *J. Mol. Catal. A* **2004**, *212*, 13−18. (j) Bianchini, C.; Mantovani, G.; Meli, A.; Migliacci, F.; Zanobini, F.; Laschi, F.; Sommazzi, A. *Eur. J. Inorg. Chem.* **2003**, 1620−1631. (k) Chen, Y. F.; Chen, R. F.; Qian, C. T.; Dong, X, C.; Sun, J. *Organometallics* **2003**, *22*, 4312−4321.

(13) (a) LePichon, L.; Stephan, D. W.; Gao, X.; Wang, Q. *Organometallics* **2002**, *21*, 1362−1366. (b) Qian, M.; Wang, M.; He, R. *J. Mol. Catal. A* **2000**, *160*, 243−247. (c) Qian, M.; Wang, M.; Zhou, B.; He, R. *Appl. Catal. A* **2001**, *209*, 11−15. (d) Bianchini, C.; Mantovani, G.; Meli, A.; Migliacci, F.; Laschi, F. *Organometallics* **2003**, *22*, 2545−2547. (e) Zhou, M.-S.; Huang, S.-P.; Weng, L.-H.; Sun, W.-H.; Liu, D.-S. *J. Organomet. Chem.* **2003**, *665*, 237−245. (f) Britovsek, G. J. P.; Gibson, V. C.; Hoarau, O. D.; Spitzmesser, S. K.; White, A. J. P.; Williams, D. J. *Inorg. Chem.* **2003**, *42*, 3454−3465.

(14) (a) Laine, T. V.; Lappalainen, K.; Liimatta, J.; Aitola, E.; Loefgren, B.; Leskelae, M. *Macromol. Rapid Commun.* **1999**, *20*, 487−491. (b) Laine, T. V.; Piironen, U.; Lappalainen, K.; Klinga, M.; Aitola, E.; Leskelae, M. *J. Organomet. Chem.* **2000**, *606*, 112−124.

(15) (a) Singer, A. W.; McElvain, S. M. *J. Am. Chem. Soc.* **1935**, *57*, 1135−1136. (b) Barnes, R. A.; Fales, H. M. *J. Am. Chem. Soc.* **1953**, *75*, 3830−3831.

Scheme 1[a]

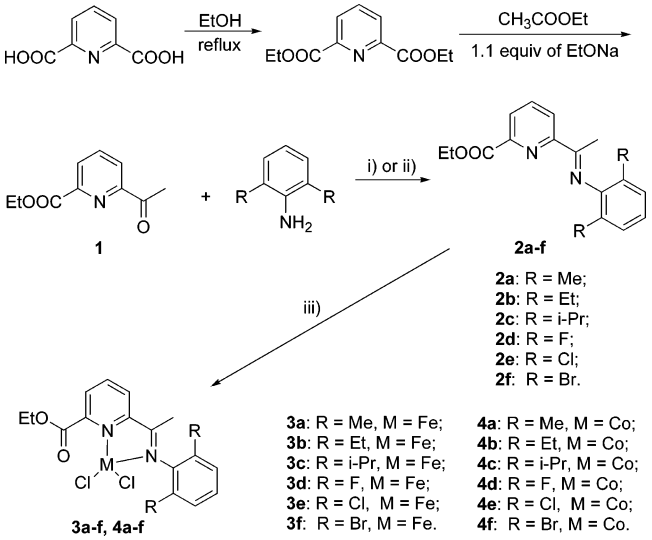

[a] Reagents and conditions: (i) ligands **2a**−**c**, toluene, *p*-TsOH; (ii) ligands **2d**−**f**, toluene, *p*-TsOH, silica−alumina catalyst support, 4 Å molecular sieves; (iii) $FeCl_2$ for complexes **3a**−**f** and $CoCl_2$ for complexes **4a**−**f** in ethanol. Note: there is a bonding interaction between iron and the carbonyl oxygen in **3b**.

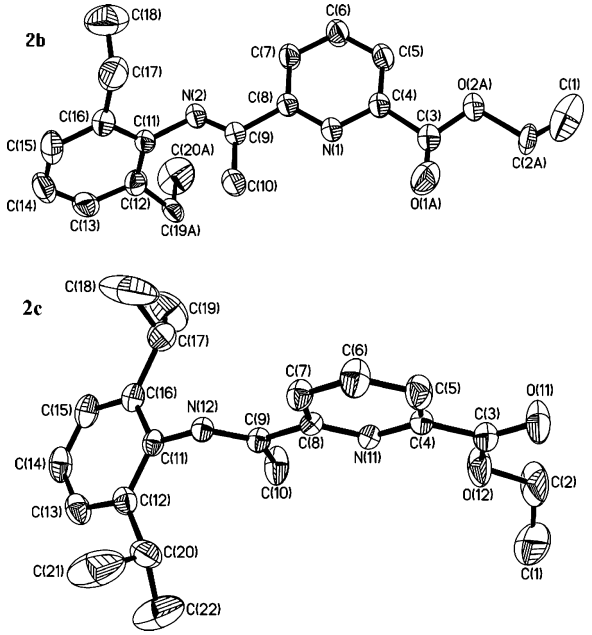

Figure 1. Molecular structure of **2b** and one of the two molecules in an asymmetric unit of **2c**. Hydrogen atoms have been omitted for clarity. Selected bond lengths (Å) and angles (deg) are as follows. **2b**: N(2)−C(9) = 1.266(3); C(9)−N(2)−C(11) = 120.3(2), N(2)−C(9)−C(8) = 117.6(2), N(1)−C(8)−C(9) = 115.7(2). **2c**: N(12)−C(9) = 1.272(3); C(9)−N(12)−C(11) = 120.7(2), N(12)−C(9)−C(8) = 116.8(2). Note: in the crystal state of **2b**, C(19) and C(20) in the disordered ethyl group, as well as C(2), O(1), and O(2) in the disordered ester group, may vibrate to another position. For clarity, only one position of these atoms is shown.

crystallographically independent, closely similar molecules in one asymmetric unit of **2c**.

The ferrous complexes **3a**−**f** were prepared by stirring an ethanol solution of anhydrous $FeCl_2$ and the corresponding pyridineimine ligands at room temperature (Scheme 1). The obtained complexes were soluble in ethanol but did not dissolve in diethyl ether. Therefore, anhydrous diethyl ether was added to precipitate the complexes. After they were washed with diethyl ether, complexes **3a**−**f** were obtained as blue powders in good yields (typically 80.0−85.0%) and high purities. These complexes are air-stable in the solid state, but the solutions of these complexes turned from blue to brown when exposed to air for a few minutes, probably due to the oxidation of Fe(II) into Fe(III). The structures of these complexes were determined by elemental analysis and IR. NMR data were not obtained, due to the paramagnetic nature of these complexes. The elemental analysis results reveal that the components of these complexes are in accord with the formula $MLCl_2$. The IR spectra of the ligands show that the C═N stretching frequencies appear in the range of 1640−1655 cm^{-1}, while the C═N stretching vibrations in complexes **3a**−**f** shift toward lower frequencies between 1619 and 1625 cm^{-1} with weak intensities. This result indicates the coordinating interaction between the imino nitrogen atom and the metal center. In addition, the slight wavenumber shift of 10−20 cm^{-1} in the C═O stretching vibrations in IR spectra suggests the presence of a weak bonding interaction between the iron and the carbonyl oxygen of the ester group in complexes **3a**−**f**.

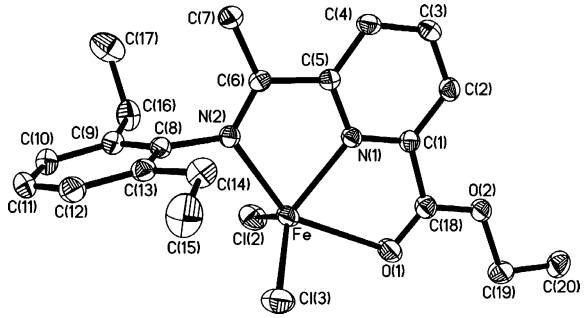

Figure 2. Molecular structure of **3b**. Hydrogen atoms have been omitted for clarity. Selected bond lengths (Å) and angles (deg): Fe−N(1) = 2.1015(15), Fe−N(2) = 2.2117(15), Fe−Cl(2) = 2.2714(7), Fe−Cl(3) = 2.2545(9), Fe−O(1) = 2.3769(15); N(1)−Fe−N(2) = 74.53(6), N(1)−Fe−Cl(3) = 125.44(5), N(2)−Fe−Cl(3) = 101.79(5), N(1)−Fe−Cl(2) = 107.25(5), N(2)−Fe−Cl(2) = 103.94(5), Cl(2)−Fe−Cl(3) = 125.72(3), N(1)−Fe−O(1) = 72.25(6), N(2)−Fe−O(1) = 146.21(5), Cl(3)−Fe−O(1) = 92.44(5), Cl(2)−Fe−O(1) = 91.72(5).

Crystals of **3b**,**c**,**e**,**f** suitable for single-crystal X-ray diffraction analysis were grown by layering pentane on a dichloromethane solution at room temperature under a nitrogen atmosphere. Crystal structures of **3b**,**c**,**e**,**f** are shown in Figures 2−5, respectively. As shown in Figure 2, the carbonyl oxygen atom in **3b** coordinates with iron. The geometry around the metal center can be described as a distorted trigonal bipyramidal with the pyridyl nitrogen atom and the two chlorine atoms forming an equatorial plane. The deviation of the iron atom from the equatorial plane is 0.160 Å. The phenyl ring is oriented perpendicularly (90.1°) to the coordination plane containing the ligand backbone and the iron atom. The C═N bond in **3b** displays clear double-bond character (1.282(2) Å) and is only 0.016 Å longer than that in the free ligand **2b**, indicating that imine is not involved in bond delocalization within the ligand backbone. The Fe−N(imino) and Fe−N(pyridyl) bond lengths

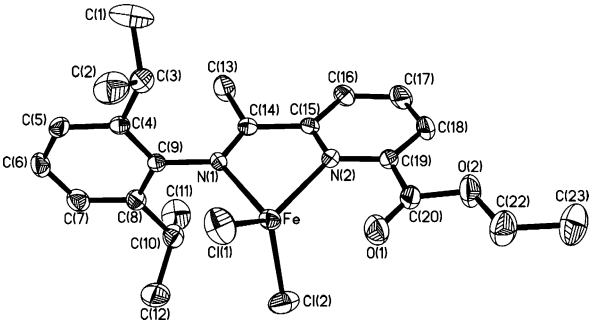

Figure 3. Molecular structure of **3c**. Hydrogen atoms have been omitted for clarity. Selected bond lengths (Å) and angles (deg): Fe−N(1) = 2.187(2), Fe−N(2) = 2.093(2), Fe−Cl(1) = 2.2187(9), Fe−Cl(2) = 2.2360(10), Fe- - -O(1) = 2.610; N(2)−Fe−N(1) = 75.85(9), N(2)−Fe−Cl(1) = 130.50(7), N(1)−Fe−Cl(1) = 106.66(7), N(2)−Fe−Cl(2) = 107.65(7), N(1)−Fe−Cl(2) = 108.49(7), Cl(1)−Fe−Cl(2) = 117.29(4), C(14)−N(1)−Fe = 115.45(19), C(15)−N(2)−Fe = 115.32(19).

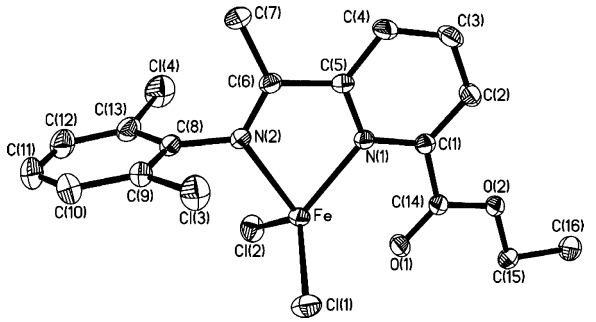

Figure 4. Molecular structure of **3e**. Hydrogen atoms and the CH_2Cl_2 solvate molecule have been omitted for clarity. Selected bond lengths (Å) and angles (deg): Fe−N(1) = 2.104(2), Fe−N(2) = 2.192(2), Fe−Cl(1) = 2.2566(10), Fe−Cl(2) = 2.2532(10), Fe- - -O(1) = 2.454; N(1)−Fe−N(2) = 74.92(8), N(1)−Fe−Cl(2) = 121.30(6), N(2)−Fe−Cl(2) = 102.46(6), N(1)−Fe−Cl(1) = 116.38(6), N(2)−Fe−Cl(1) = 108.15(6), Cl(2)−Fe−Cl(1) = 119.62(4).

(2.2217(15) and 2.1015(15) Å, respectively) are similar to the corresponding Fe−N bond lengths of diisopropyl 2,6-bis(imino)pyridyl ferrous complexes reported by Brookhart et al.[4a] It is noted that the Fe−O(1) bond length (2.3769(15) Å) is substantially longer than the reported Fe−O bond distance (2.212(4) Å),[16] which indicates the weak interaction between the iron and carbonyl oxygen atom in **3b**.

Figure 3 shows that the iron atom is coordinated in a distorted-tetrahedral environment in **3c**. The diisopropyl-substituted phenyl ring is oriented nearly perpendicular to the coordination plane, and the dihedral angle is 86.5°. Similarly, complexes **3e**,**f** are four-coordinated with a distorted-tetrahedral geometry around the metal center. One dichloromethane molecule was observed in the crystal lattices of **3e**,**f**. The phenyl rings in **3e**,**f** are oriented orthogonally to the coordination rings (88.9 and 89.0°, respectively). The Fe−N(imino) bond lengths in **3c**,**e**,**f** (2.187(2), 2.192(2), and 2.197(3) Å, respectively) are slightly shorter than that in pentacoordinated **3b**, reflecting the subtle effect of the coordination fashion on the electronic properties of the metal center. It should be pointed out that the oxygen atom in the carbonyl

(16) Chiou Y.-M.; Que, L., Jr. *J. Am. Chem. Soc.* **1995**, *117*, 3999−4013.

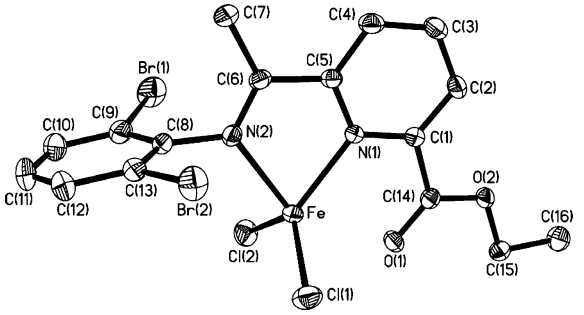

Figure 5. Molecular structure of **3f**. Hydrogen atoms and the CH_2Cl_2 solvate molecule have been omitted for clarity. Selected bond lengths (Å) and angles (deg): Fe−N(1) = 2.103(3), Fe−N(2) = 2.197(3), Fe−Cl(2) = 2.2453(13), Fe−Cl(1) = 2.2548(13), Fe- - -O(1) = 2.452; N(1)−Fe−N(2) = 74.48(11), N(1)−Fe−Cl(2) = 121.74(9), N(2)−Fe−Cl(2) = 102.89(8), N(1)−Fe−Cl(1) = 115.06(9), N(2)−Fe−Cl(1) = 109.25(9), Cl(2)−Fe−Cl(1) = 120.04(5).

group orients toward the iron center in **3c**,**e**,**f**, and the distances between oxygen and iron are 2.610, 2.454, and 2.452 Å, respectively, which are slightly longer than the Fe−O(1) bond length in **3b**. A perusal of the bond angles around the metal center of complexes **3c**,**e**,**f** shows that their coordination geometries are greatly distorted from an idealized tetrahedron, which may be attributable to the effect of the carbonyl oxygen atom on the coordination environment.

The cobaltous complexes **4a**−**f** were conveniently prepared via stirring an ethanol solution of anhydrous $CoCl_2$ and the corresponding ligands (Scheme 1). These complexes were obtained as green powders in good yields (63.0−73.4%) and are stable in both solution and the solid state. The structures of the complexes were characterized by elemental analysis and IR spectroscopy. Similar to the ferrous complexes, all the cobaltous complexes show lowered frequencies of ν(C═N) with wavenumber shifts of 20−30 cm^{-1} and decreased intensity in their IR spectra, relative to the corresponding ligands. Attempts to characterize these complexes by NMR failed due to the paramagnetism of these complexes.

Crystals of complex **4c** suitable for X-ray diffraction were grown by slowly diffusing diethyl ether into a dichloromethane solution (Figure 6). Complex **4c** has the same distorted-tetrahedral geometry as its ferrous analogue **3c**. The sterically bulky isopropyl groups hold the N-aryl ring nearly perpendicular to the plane of the coordinated ring (85.9°), which may provide efficient blocking of the axial sites on the cobalt center. Crystals of **4f** suitable for X-ray determination were obtained by layering its dichloromethane solution with diethyl ether (Figure 7). One dichloromethane molecule was found to be involved in the crystal lattice, as revealed by an X-ray determination. Complex **4f** is four-coordinated with a distorted-tetrahedral geometry around the central metal. The phenyl ring is oriented nearly perpendicular to the coordination ring, and the dihedral angle is 89.5°. Similar to the four-coordinated ferrous complexes, the oxygen in the carbonyl group in complex **4f** orients toward the metal center, and the distance between them is 2.460 Å.

2. Ethylene Oligomerization and Polymerization. 2.1. Ethylene Oligomerization and Polymerization Behavior of the Ferrous Complexes. The

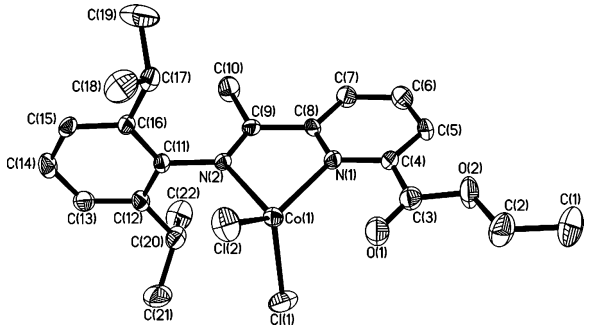

Figure 6. Molecular structure of **4c**. Hydrogen atoms have been omitted for clarity. Selected bond lengths (Å) and angles (deg): Co(1)−N(1) = 2.039(3), Co(1)−N(2) = 2.133(3), Co(1)−Cl(1) = 2.2240(12), Co(1)−Cl(2) = 2.2020(12), Co- - -O(1) = 2.610; N(1)−Co(1)−N(2) = 77.81(12), N(1)−Co(1)−Cl(2) = 131.35(9), N(2)−Co(1)−Cl(2) = 107.11(9), N(1)−Co(1)−Cl(1) = 109.60(8), N(2)−Co(1)−Cl(1) = 109.01(8), Cl(2)−Co(1)−Cl(1) = 113.67(5).

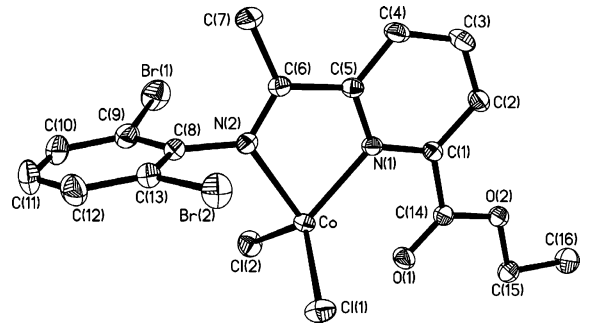

Figure 7. Molecular structure of **4f**. Hydrogen atoms and the CH_2Cl_2 solvate molecule have been omitted for clarity. Selected bond lengths (Å) and angles (deg): Co−N(1) = 2.050(3), Co−N(2) = 2.126(3), Co−Cl(1) = 2.2316(15), Co−Cl(2) = 2.2316(15), Co- - -O(1) = 2.460; N(1)−Co−N(2) = 77.27(13), N(1)−Co−Cl(2) = 122.43(11), N(2)−Co−Cl(2) = 103.97(10), N(1)−Co−Cl(1) = 116.07(11), N(2)−Co−Cl(1) = 117.20(6), Cl(2)−Co−Cl(1) = 117.20(6).

ferrous complexes **3a**−**f** were initially studied for their catalytic activities of ethylene oligomerization and polymerization using methyaluminoxane (MAO) as the cocatalyst. The results are summarized in Table 1 with 1 atm of ethylene and in Table 2 with 10 atm of ethylene.

Effect of the Ligand Environment on the Catalytic Behavior. Complexes **3a**−**f** show considerable activities for ethylene oligomerization at a pressure of 1 atm of ethylene, producing butenes and hexenes and small amounts of higher oligomers. In addition, the catalytic systems **3a**,**b** generate isolable amounts of polyethylene. A variety of ortho-substituted aryl-ring-containing ligands were employed, including electron-donating alkyl groups and electron-withdrawing halogen groups, and the studies of these complexes have provided an insight into the steric and electronic effects of the aryl ring on the catalytic behaviors of the complexes, including the catalytic activity and product distribution. The ethylene catalytic results for complexes **3a**−**f** were obtained under identical reaction conditions and are listed in entries 1−6 in Table 1. As shown in Table 1, the ethylene oligomerization activity varies in the orders of **3a** > **3b** > **3c** and **3e** > **3d** > **3f**, and a similar trend of polymerization activity was observed for the alkyl-substituted complexes **3a**−**c**. The explanation for these results is based upon the steric bulk of the substituent on the ortho position of the aryl ring that decreasing the bulk on the aryl ring of the complex leads to higher activity, which is in line with previous reports regarding bis(imino)pyridyl iron catalysts.[7,11j] Complex **3e**, with dichloro-substituted ligands, displays higher ethylene oligomerization activity than its analogue **3d**, which contains difluoro-substituted ligands, and the same result was obtained for the cobaltous counterparts. From the point of view of electronic effects, fluoro substitution on the ortho position of the aryl ring results in a more electrophilic metal center, which may increase the catalytic activity of the complex for ethylene oligomerization and polymerization.[17] However, the less bulky fluoro substituent renders the active sites of the catalyst exposed to not only ethylene but also other reactive species, and the latter actually leads to the deactivation of the active species. Indeed, Gibson has shown that the catalytic intermediates formed from the precursors containing pyridyldiimine ligands which lack sufficient steric bulk in the ortho aryl positions are more easily deactivated through the interaction with alkylaluminum reagent.[12h] Although electronic effects on the activities of catalysts were emphasized in previous studies,[12d,k] our results clearly indicate that the electronic effect is not significant in the catalyst systems we studied. In addition, the five-coordinate nature of **3b** in the solid state has little effect on its ethylene catalytic behavior, and in solution, the coordination mode of **3b** may change to four-coordinate due to the weak Fe−O bond. In the literature, an N∧N∧O-coordinated ferrous complex bearing an acetyliminopyridine ligand shows much lower catalytic activity for ethylene oligomerization than the corresponding bis(imino)pyridine complex.[12i]

The effect of the steric bulk on the oligomer distribution is not as remarkable as the effect on the catalytic activity, and no conclusive trend can be determined. Analysis of the obtained oligomers by GC and GC-MS reveals that the selectivities for linear α-olefin are higher than 93% in all cases at 1 atm of ethylene.

Effects of Al/Fe Molar Ratio and Reaction Temperature on Catalyst Activity. The influences of the Al/Fe molar ratio and the reaction temperature on ethylene oligomerization and polymerization were investigated in detail with complex **3c**. Increasing the Al/Fe molar ratio from 200 to 1500 leads to a slight enhancement of complex **3c**'s ethylene oligomerization activity (entries 3 and 7−9 in Table 1). Elevation of the ethylene oligomerization and polymerization reaction temperature from 0 to 40 °C results in a sharp decrease in productivity, which may be attributed to catalyst decomposition and lower ethylene solubility at higher temperature.[12a,h]

Solvent Effect on the Catalyst Activity. The effect of solvent on the catalytic activity was studied with complex **3f**. As shown in Table 1, **3f** exhibits about a 4 times higher activity of ethylene oligomerization in dichloromethane (entry 13) than in toluene (entry 6). The obtained oligomers were analyzed by GC and GC-MS, and only the dimers were detected. The selectivity for 1-butene is higher than 97%.

(17) (a) Chan, M. S. W.; Deng, L. Q.; Ziegler, T. *Organometallics* **2000**, *19*, 2741−2750. (b) Zhang, T. Z.; Sun, W.-H.; Li, T.; Yang, X. Z. *J. Mol. Catal. A* **2004**, *218*, 119−124.

Table 1. Polymerization and Oligomerization of 1 atm of Ethylene with 3a−f/MAO[a]

				oligomer distribn[b] (%)				activity (10^4 g (mol of Fe)$^{-1}$ h^{-1})	
entry	complex	Al/Fe (mol)	temp (°C)	$C_4/\sum C$	$C_6/\sum C$	$C_{\geq 8}/\sum C$	linear α-olefin	oligomer[b]	polymer
1	**3a**	1000	15	92.40	4.25	3.35	>99	2.17	9.44
2	**3b**	1000	15	71.15	28.84		97.1	1.61	0.91
3	**3c**	1000	15	98.20	1.50	0.3	>99	1.39	trace
4	**3d**	1000	15	84.04	0.90	15.06	94.6	2.60	no
5	**3e**	1000	15	35.42	57.74	6.84	97.7	6.04	trace
6	**3f**	1000	15	77.96	2.89	19.15	93.3	1.80	trace
7	**3c**	200	15				>99	0.76	no
8	**3c**	500	15				97.2	1.15	trace
9	**3c**	1500	15				>99	2.46	trace
10	**3c**	1000	0				>99	6.98	trace
11	**3c**	1000	40				>99	0.66	no
12	**3c**	1000	60				>99	0.48	no
13[c]	**3f**	1000	15	100[d]			97.8	7.18[d]	no
14[e]	**3f**	1000	15	100			>99	2.45	no

[a] General conditions: 5 μmol of precatalyst; 30 mL of toluene; reaction time 30 min. [b] Determined by GC. ∑C means the total amounts of oligomers. [c] CH_2Cl_2 as solvent. [d] Determined by GC and GC-MS; approximate result. [e] 2 equiv of PPh_3 as auxiliary ligand.

Table 2. Oligomerization and Polymerization of 10 atm of Ethylene with 3a−f/MAO[a]

	complex	polymer	activity (10^4 g (mol of Fe)$^{-1}$ h^{-1})					linear	
entry	(amt (μmol))	yield (g)	oligomer[b]	polymer	M_n[c] (10^3)	PDI[c]	T_m[d] (°C)	α-olefin (%)	K
1	**3a** (42.3)	24.00	6.20	56.70	4.7	32.7	132	88.8	0.83
2	**3b** (53.9)	1.15	1.44	2.10	1.3	90.3	122	82.1	0.93
3	**3c** (36.5)	1.13	1.90	3.20	1.0	4.2	124	92.1	0.96
4	**3d** (34.1)	trace	4.06					78.3	0.73
5[e]	**3e** (42.5)	1.67	30.60	3.90	0.5	2.4	88	92.0	0.81
6	**3f** (36.9)	3.50	3.90	9.50	0.7	2.4	110	95.8	0.81

[a] General conditions: Al/Fe molar ratio 1000; 20 °C; 1 h, 700 mL of toluene. [b] Determined by GC. [c] Determined by GPC. [d] Determined by DSC. [e] The oligomers were determined by GC and GC-MS.

Effect of the Auxiliary Ligand on Catalyst Activity. Previous studies on nickel-based catalysts have demonstrated that incorporating PPh_3 into catalytic systems leads to higher activity and longer catalyst lifetime.[7g,18] We were curious whether such effects would apply to our ferrous catalyst systems. Therefore, the oligomerization reaction with the **3f**/MAO system was carried out in the presence of 2 equiv of PPh_3 (entry 14, Table 1). However, as shown in Table 1, only a slight increase of catalyst activity was observed relative to the catalytic system of **3f**/MAO (entry 6, Table 1).

Effects of Ethylene Pressure on the Catalyst Behavior. Ethylene oligomerization and polymerization with complexes **3a**−**f** in the presence of MAO were also studied under an ethylene pressure of 10 atm, and the results are listed in Table 2. As is apparent, the ethylene concentration significantly affects the catalytic behaviors of the complexes. For the alkyl-substituted ferrous complexes **3a**−**c**, the effects of the steric bulk of the ortho aryl substituent on the catalyst's ethylene polymerization activities at 10 atm of ethylene pressure are quite consistent with those observed at 1 atm of ethylene. As shown in Table 2 (entries 1−3), higher polymerization activity was observed for the complex containing a ligand with less bulky substituents. In addition, the dibromo-substituted complex **3f** shows higher polymerization activity and lower oligomerization activity than the dichloro-substituted complex **3e**.

In comparison with the results obtained with 1 atm of ethylene, the distribution of oligomers formed at 10 atm of ethylene pressure shifts to higher carbon number olefins. Figure 8 shows the distributions of the oligomers

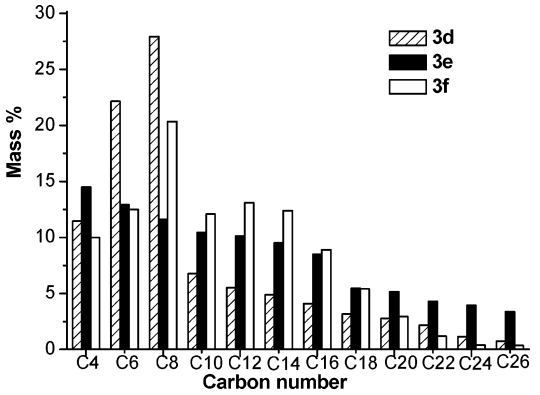

Figure 8. Oligomer distribution obtained in entries 4−6 in Table 2.

obtained with the catalytic systems of **3d**−**f** under 10 atm of ethylene. The distribution of olefin oligomers follows the Schulz−Flory rules[19] and is characterized by the constant K as defined in eq 1, where K represents

$$K = k_{prop}/(k_{prop} + k_{ch-transfer}) = \text{(mol of } C_{n+2} \text{ oligomers)/(mol of } C_n \text{ oligomers)} \quad (1)$$

the probability of chain propagation. The K values determined by the molar ratio of C_{14} and C_{16} fractions for each run are listed in Table 2. As shown in Table 2, increasing the bulk at the ortho position of the aryl group on the complex leads to an increase in the K value (entries 1−3 in Table 2). GC and GC-MS analysis of the oligomers indicates that the selectivities for linear α-olefins are higher than 78% for **3a**−**f** at 10 atm of ethylene.

(18) (a) Carlini, C.; Isola, M.; Liuzzo, V.; Galletti, A. M. P.; Sbrana, G. *Appl. Catal. A: Gen.* **2002**, *231*, 307−320. (b) Jenkins, J. C.; Brookhart, M. *Organometallics* **2003**, *22*, 250−256.

(19) (a) Flory, P. J. *J. Am. Chem. Soc.* **1940**, *62*, 1561−1565. (b) Schulz, G. V. Z. *Phys. Chem. B* **1935**, *30*, 379−399. (c) Schulz, G. V. Z. *Phys. Chem. B* **1939**, *43*, 25−46.

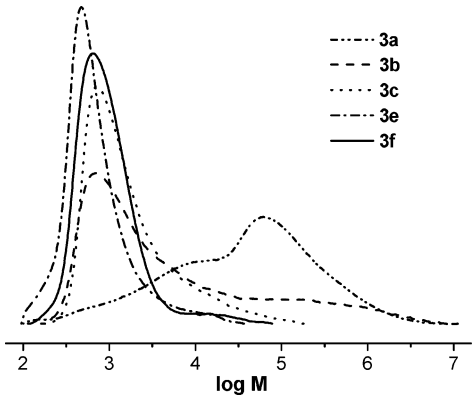

Figure 9. GPC traces of PE samples obtained in entries 1, 2, 3, 5, and 6 in Table 2.

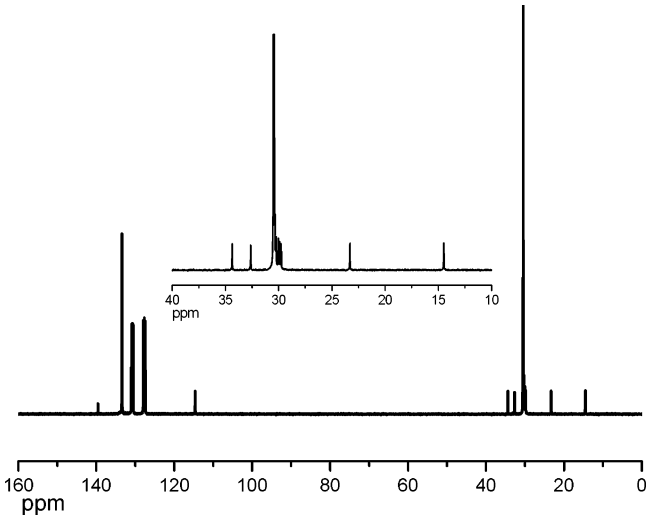

Figure 10. ^{13}C NMR spectra of the PE sample obtained in entry 5 in Table 2.

The polyethylene produced by **3a**−**c**,**e**,**f** was isolated as a white powder. The GPC analysis indicates that the obtained polyethylene has a relatively low molecular weight, with the M_n value in the range of 500−4700. As shown by the GPC traces in Figure 9, the PE samples obtained from **3a**,**b** display bimodal molecular weight distribution. The observed bimodal distribution is attributed to the formation of the different types of active species when the complexes are activated by MAO and the rate difference between chain transfer and chain propagation of these active species. The M_n value of the PE produced by **3a** is much higher than those obtained from **3b**,**c**, which is surprising in view of previous reports,[4a,12h] which demonstrated a higher molecular weight for PE produced with a ligand of greater steric bulk. However, in our study, repeated ethylene polymerization reactions with **3a**−**c** under 10 atm demonstrate consistent results for both the catalyst activity and the molecular weight of the obtained PE. In addition, the PE produced by dihalogen-substituted complexes **3e**,**f** has a lower M_n value than the PE produced by dialkyl-substituted **3a**−**c**. Analysis of the product by ^1H NMR and ^{13}C NMR shows that the PE samples are strictly linear and the end groups are mainly α-olefin.[20] The ^{13}C NMR spectra for the PE sample listed in entry 5 of Table 2 is shown in Figure 10. Furthermore, the IR spectroscopic analysis of the obtained PE confirms the presence of end vinyl groups, which implies that chain termination occurs with β-hydride elimination for the polymeric α-olefin. The M_n value calculated from ^1H NMR and ^{13}C NMR spectra for the PE sample generated by **3e** is approximately 700, which is slightly higher than that obtained by GPC. However, the M_n value obtained from NMR may be more accurate, due to the fact that GPC may afford an ambiguous characterization of low-molecular-weight polyethylene.[6d] Moreover, DSC studies determine that the T_m values of the PE samples are in the range of 88−132 °C, which correlates well with the linear characteristics of low-molecular-weight PE.

2.2. Ethylene Oligomerization and Polymerization Behaviors of the Cobaltous Complexes. The cobaltous complexes **4a**−**f** were systematically investigated for their ethylene oligomerization and polymerization behavior upon activation with MAO, and the results are summarized in Table 3 (with 1 atm of ethylene) and Table 4 (with 10 atm of ethylene). Previous studies on the 2,6-bis(imino)pyridine-based iron and cobalt catalyst systems demonstrated that cobalt complexes usually display much lower productivity than iron complexes.[12h,j,k] However, the cobaltous catalysts in our study exhibit remarkably higher ethylene oligomerization activities than their ferrous counterparts at 1 atm. We noted rapid consumption of ethylene in the experiments when MAO was injected into the catalytic systems, which indicates that no initial time of ethylene oligomerization and polymerization is required. GC and GC-MS analysis of the obtained oligomers reveals that dimers and trimers are the major products, plus a small amount of higher carbon number olefins, and the linear α-olefins are the predominant products.

Effects of the Aryl Substituents on the Catalyst Behaviors. The ligand environment has a significant effect on productivity. The less bulky methyl-substituted complex **4a** displays higher total conversion of ethylene than the sterically bulky isopropyl-substituted complex **4c**. Nevertheless, **4c** produces more polyethylene than **4a** under identical reaction conditions (Table 3, entry 1 vs entry 9). In addition, the dibromo-substituted complex **4f** generates a trace amount of polyethylene, while the difluoro-substituted complex **4d** and the dichloro-substituted complex **4e** produce only oligomers (Table 3, entries 10, 11, and 15). The effect of aryl substituents on the cobaltous complexes' catalytic behavior is well in line with the reported result.[4a,12d,h] Similar to the results obtained with the ferrous complexes, the electronic effect on the catalyst productivity is not significant.

Effects of Al/Co Molar Ratio and Reaction Temperature on Catalyst Activity. The Al/Co molar ratio slightly affects the oligomerization and polymerization activity of complex **4b**. Complex **4b** shows the highest activity when the Al/Co ratio is 1000 (Table 3, entries 2−5). For complexes **4b**,**f**, increasing the reaction temperature in the range of −10 to +40 °C leads to reduced oligomerization activities, suggesting that the active species may be less stable at higher temperature.

(20) (a) Kokko, E.; Lehmus, P.; Leino, R.; Luttikhedde, H. J. G.; Ekholm, P.; Näsman, J. H.; Seppälä, J. V. *Macromolecules* **2000**, *33*, 9200−9204. (b) Galland, G. B.; Quijada, R.; Rolas, R.; Bazan, G.; Komon, Z. J. A. *Macromolecules* **2002**, *35*, 339−345.

Table 3. Polymerization and Oligomerization of 1 atm of Ethylene with 4a−f/MAO[a]

					oligomer distribn[b] (%)				activity (10^4 g (mol Co)$^{-1}$ h^{-1})	
entry	complex	Al/Co (mol)	temp (°C)	time (min)	$C_4/\sum C$	$C_6/\sum C$	$C_{\geq 8}/\sum C$	linear α-olefin	oligomer[b]	polymer
1	**4a**	1000	15	30	81.80	15.27	2.93	96.2	14.70	0.670
2	**4b**	200	15	30	67.37	15.96	16.68	90.3	4.71	trace
3	**4b**	500	15	30	61.03	20.13	18.84	95.9	6.95	1.04
4	**4b**	1000	15	30	74.25	14.89	10.86	75.0	8.22	1.04
5	**4b**	1500	15	30	78.98	13.06	7.96	83.2	8.10	trace
6	**4b**	1000	−10	30	76.56	19.33	4.11	83.2	19.50	trace
7	**4b**	1000	0	30	72.97	21.46	5.57	95.6	13.05	0.972
8	**4b**	1000	40	30	67.84	18.71	13.45	89.0	3.58	trace
9	**4c**	1000	15	30	55.34	27.17	17.49	98.1	5.32	3.50
10	**4d**	1000	15	30	93.28	1.39	5.33	78.6	7.98	no
11	**4e**	1000	15	30	83.76	1.79	4.95	82.0	14.50	no
12[c]	**4e**	1000	15	30	100[d]	-	-	96.8	135.00[d]	no
13	**4f**	1000	−10	30	70.00	24.47	5.53	90.4	36.20	trace
14	**4f**	1000	0	30	66.00	24.10	9.90	94.7	24.70	trace
15	**4f**	1000	15	30	72.11	23.78	4.10	95.6	18.90	trace
16	**4f**	1000	40	30	66.86	19.27	13.86	81.5	4.42	trace
17	**4f**	1000	15	15	71.67	22.57	5.79	87.1	34.90	trace
18[c]	**4f**	1000	15	30	100[d]		-	92.8	46.90[d]	trace
19[e]	**4f**	1000	15	60	72.24	22.74	5.03	90.0	9.92	trace
20[f]	**4f**	1000	15	15	73.83	20.57	5.60	87.5	16.60	no
21[f]	**4f**	1000	15	30	71.28	23.28	5.23	92.2	31.70	no

[a] General conditions: 5 μmol of precatalyst; 30 mL of toluene. [b] Determined by GC. ∑C signifies the total amounts of oligomers. [c] CH_2Cl_2 as solvent. [d] Determined by GC and GC-MS; approximate result. [e] Determined by GC-MS. [f] 2 equiv of PPh_3 as auxiliary ligand.

Table 4. Oligomerization and Polymerization of 10 atm of Ethylene with 4c and 4f[a]

			activity (10^4 g (mol of Co)$^{-1}$ h^{-1})					
entry	complex (amt (μmol))	polymer yield (g)	oligomer[b]	polymer	M_n[c] ($\times 10^3$)	linear α-olefin (%)	PDI[c]	T_m[d] (°C)
1	**4c** (32.8)	0.18	3.63	0.53	1.9	84.6	36.4	125
2	**4f** (49.6)	0.44	23.40	0.90	1.7	97.9	16.7	125

[a] General conditions: Al/Fe molar ratio 1000; 20 °C, 1 h, 700 mL of toluene. [b] Determined by GC. [c] Determined by GPC. [d] Determined by DSC.

Lifetime of the Active Catalytic Species. All the cobaltous catalysts have been found to show very short lifetimes even at low temperature. As an example, the lifetime of **4f/MAO** was studied by varying the reaction time, and it was found that the oligomerization activity of **4f** at 30 min of reaction (Table 3, entry 15) was about half of that at 15 min of reaction (Table 3, entry 17), indicating that the majority of active catalytic species were deactivated after 15 min of reaction.

Auxiliary Ligand and Solvent Effects on the Catalyst Behavior. Oligomerization activities of the cobaltous complexes were also studied in the presence of 2 equiv of PPh_3. The results show that addition of PPh_3 to the reaction has no significant impact on the activity of **4f**/MAO. It is noted that the oligomerization activity of **4f** in the presence of PPh_3 remains high when the reaction time is prolonged from 15 to 30 min (Table 3, entries 20 and 21). The prolonged catalyst lifetime may be ascribed to the formation of more stable catalytic intermediates with the addition of PPh_3. Solvent effects on ethylene oligomerization were also investigated with **4e**,**f**. As shown in Table 3, using dichloromethane as the solvent leads to a significant increase of the oligomerization activities of **4e**,**f**, and as determined by GC and GC-MS, only butenes were detected when dichloromethane was employed as the solvent (Table 3, entries 12 and 18).

Ethylene Pressure Effects on Catalyst Performance. Cobaltous complexes **4c**,**f** were studied for ethylene oligomerization and polymerization under 10 atm of ethylene with MAO activation (Table 4). It is observed that the activity of **4c**,**f** does not change significantly with the ethylene pressure. **4c**,**f** both produce PE with low molecular weight. In addition, the molecular weight distributions of the obtained PE are considerably wide, which is characterized by a broad peak in the GPC trace (Figure 11). The polymers display T_m values of 125 °C, as measured by DSC. The IR spectra of the PE samples produced by **4c**,**f** to some extent demonstrate the PE's linear characteristics and the presence of the vinyl end groups. Further analysis of the PE was not performed, due to the low polymer productivity.

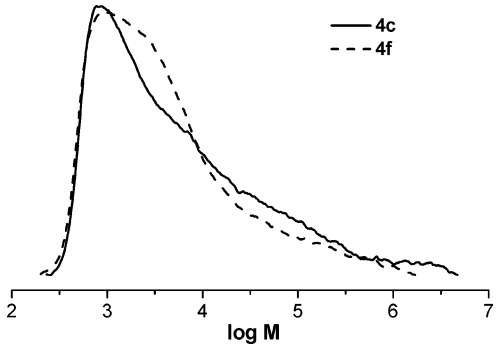

Figure 11. GPC traces of the PE samples obtained by **4c**,**f** at 10 atm.

Summary

A series of 2-(carboxylato)-6-iminopyridine-based ferrous and cobaltous complexes have been synthesized. In the presence of MAO, these complexes exhibit good activities for oligomerization and polymerization. The steric bulk dependence of the activities was observed

for both the ferrous and cobaltous catalyst systems. A decrease in the steric bulk of the substituent on the ligand leads to a higher activity of the catalyst, except for the difluoro-substituted complexes. The electronic effects on the catalytic activities are less significant. The cobaltous complexes **4a**−**f** display very short lifetimes, due to deactivation of the active catalytic sites. Analysis of the products shows that the majority of obtained oligomers are linear α-olefins, and the polymers obtained in some cases are linear polymeric α-olefins.

Experimental Section

General Considerations. All manipulations of air- and/or moisture-sensitive compounds were performed under a nitrogen atmosphere using standard Schlenk techniques. Solvents were dried by the literature methods. Methylaluminoxane (MAO) was purchased from Albemarle as a 1.4 M solution in toluene. Other reagents were purchased from Aldrich or Acros Chemicals. ^{1}H and ^{13}C NMR spectra were recorded on a Bruker DMX 300 MHz instrument at ambient temperature using TMS as an internal standard. IR spectra were recorded on a Perkin-Elmer System 2000 FT-IR spectrometer. Elemental analysis was carried out using an HP-MOD 1106 microanalyzer. GC analysis was performed with a Carlo Erba Strumentazione gas chromatograph equipped with a flame ionization detector and a 30 m (0.25 mm i.d., 0.25 μm film thickness) DM-1 silica capillary column. GC-MS analysis was performed with HP 5890 SERIES II and HP 5971 SERIES mass detectors. The yield of oligomers was calculated by referencing with the mass of the solvent on the basis of the prerequisite that the mass of each fraction is approximately proportional to its integrated areas in the GC trace. Selectivity for the linear α-olefin is defined as (amount of linear α-olefin of all fractions)/(total amount of oligomer products) in percent. ^{1}H and ^{13}C NMR spectra of the PE samples were recorded on a Bruker DMX 400 MHz instrument at 135 °C in 1,2-dichlorobenzene-d_4 using TMS as the internal standard. The molecular weight and polydispersity index (PDI) of PE were determined by a PL-GPC220 instrument at 150 °C with 1,2,4-trichlorobenzene as the eluent. Melting points of the polymers were obtained on a Perkin-Elmer DSC-7 instrument in the standard DSC run mode. The instrument was initially calibrated for the melting point of an indium standard at a heating rate of 10 °C/min. The polymer sample was first equilibrated at 0 °C and then heated to 160 °C at a rate of 10 °C/min to remove thermal history. The sample was then cooled to 0 °C at a rate of 10 °C/min. A second heating cycle was used for collecting DSC thermogram data at a ramping rate of 10 °C/min.

Synthesis of Ethyl 6-Acetylpyridine-2-carboxylate (1). According to the traditional method, 2,6-dicarbethoxypyridine was prepared by the esterification of dipicolinic acid with ethanol with a yield of 70%. Mp: 41.0−41.5 °C. A solution of 2,6-dicarbethoxypyridine (18.9 g, 0.085 mol) in 70 mL of freshly distilled ethyl acetate was added dropwise to 1.1 equiv of dried C_2H_5ONa (6.4 g, 0.094 mol) with stirring to afford a yellow mixture, which was refluxed for 12 h and then allowed to stand overnight. Concentrated HCl (35 mL) was added dropwise with stirring, and the mixture was refluxed for a period of 6 h to complete the reaction. Water (100 mL) was then added, and the mixture turned orange. The aqueous phase was extracted with CH_2Cl_2 (4 × 25 mL), and the combined extract was washed with 5% aqueous Na_2CO_3. The combined organic phase was dried over anhydrous Na_2SO_4 and filtered, and the solvent was evaporated under reduced pressure. The desired compound 6-acetylpyridine-2-carboxylate (**1**) was obtained as a white solid in 40.0% yield after purification by column chromatography (silica gel, petroleum ether/ethyl acetate 8/1). Mp: 50.0−51.5 °C. ^{1}H NMR (300 MHz, $CDCl_3$; δ): 8.27 (q, 1H, J_1 = 1.2 Hz, J_2 = 6.6 Hz, Py H_m); 8.20 (q, 1H, J_1 = 1.2 Hz, J_2 = 6.6 Hz, Py H_m); 7.99 (t, 1H, J = 7.8 Hz, Py H_p); 4.50 (q, 2H); 2.81 (s, 3H); 1.47 (t, 3H). ^{13}C NMR (75.45 MHz, $CDCl_3$; δ): 199.72; 164.70; 153.61; 147.85; 138.01; 128.16; 124.43; 62.12; 25.71; 14.33. IR (KBr; cm^{-1}): 1727 ($\nu_{C=O}$); 1704; 1585; 1474; 1455; 1321; 1367; 1237; 1155. Anal. Calcd for $C_{10}H_{11}NO_3$: C, 62.17; H, 5.74; N, 7.25. Found: C, 62.14; H, 5.75; N, 7.17.

Synthesis of Ligands. Ethyl 6-[1-((2,6-Dimethylphenyl)imino)ethyl]pyridine-2-carboxylate (2a). A solution of 2,6-dimethylaniline (0.267 g, 2.2 mmol), ethyl 6-acetylpyridine-2-carboxylate (0.386 g, 2.0 mmol), and a catalytic amount of *p*-toluenesulfonic acid in toluene (25 mL) were refluxed for 24 h. After solvent evaporation, the crude product was purified by column chromatography on silica gel with petroleum ether/ethyl acetate (15/1) as eluent to afford the product as a yellow powder in 69.5% yield. ^{1}H NMR (300 MHz, $CDCl_3$; δ): 8.58 (d, 1H, J = 7.9 Hz, Py H_m); 8.20 (d, 1H, J = 7.6 Hz, Py H_m); 7.95 (t, 1H, J = 7.9 Hz, Py H_p); 7.07 (d, 2H, J = 7.4 Hz, Ar *H*); 6.95 (t, 1H, J = 7.4 Hz, Ar *H*); 4.49 (q, 2H); 2.26 (s, 3H); 2.03 (s, 6H); 1.46 (t, 3H, J = 7.1 Hz). ^{13}C NMR (75.45 MHz, $CDCl_3$; δ): 166.98; 165.15; 156.45; 148.57; 147.39; 137.32; 126.16; 125.27; 124.33; 123.18; 61.88; 17.92; 16.51; 14.31. IR (KBr; cm^{-1}): 1720 ($\nu_{C=O}$); 1640 ($\nu_{C=N}$); 1587; 1469; 1370; 1324. Anal. Calcd for $C_{18}H_{20}N_2O_2$: C, 72.95; H, 6.80; N, 9.45. Found: C, 72.46; H, 6.77; N, 9.29.

Ethyl 6-[1-((2,6-Diethylphenyl)imino)ethyl]pyridine-2-carboxylate (2b). Using the same procedure as for the synthesis of **2a**, **2b** was obtained as a yellow powder in 68.2% yield. ^{1}H NMR (300 MHz, $CDCl_3$; δ): 8.49 (d, 1H, J = 7.8 Hz, Py H_m); 8.12 (d, 1H, J = 7.5 Hz, Py H_m); 7.87 (t, 1H, J = 7.8 Hz, Py H_p); 7.15 (d, 2H, J = 7.5 Hz, Ar *H*); 6.96 (t, 1H, J = 6.3 Hz, Ar *H*); 4.42 (q, 2H); 2.71 (m, 4H); 2.18 (s, 3H); 1.39 (t, 3H); 1.05 (t, 6H). ^{13}C NMR (75.45 MHz, $CDCl_3$; δ): 166.66; 165.17; 156.43; 147.57; 147.38; 137.31; 131.03; 126.11; 125.94; 124.26; 123.45; 61.87; 24.54; 16.81; 14.29; 13.67. IR (KBr; cm^{-1}): 1722 ($\nu_{C=O}$); 1640 ($\nu_{C=N}$); 1580; 1540; 1454; 1394. Anal. Calcd for $C_{20}H_{24}N_2O_2$: C, 74.04; H, 7.46; N, 8.64. Found: C, 73.95; H, 7.49; N, 8.52.

Ethyl 6-[1-((2,6-Diisopropylphenyl)imino)ethyl]pyridine-2-carboxylate (2c). Using the same procedure as for the synthesis of **2a**, **2c** was obtained as a yellow powder in 71.5% yield. ^{1}H NMR (300 MHz, $CDCl_3$; δ): 8.56 (d, 1H, J = 7.8 Hz, Py H_m); 8.19 (d, 1H, J = 7.5 Hz, Py H_m); 7.93 (t, 1H, J = 7.8 Hz, Py H_p); 7.15 (q, 1H, J_1 = 6.3 Hz, J_2 = 2.1 Hz, Ar *H*); 7.10 (q, 1H, J_1 = 6.0 Hz, J_2 = 3.0 Hz, Ar *H*); 7.04 (t, 1H, J = 7.8 Hz, Ar *H*); 4.48 (q, 2H); 2.71 (m, 2H); 2.28 (s, 3H); 1.45 (t, 3H); 1.36 (t, 12H). ^{13}C NMR (75.45 MHz, $CDCl_3$; δ): 166.67; 165.19; 156.40; 147.39; 146.24; 137.31; 135.64; 126.10; 124.31; 123.71; 123.00; 61.87; 28.24; 23.22; 17.11; 14.28. IR (KBr; cm^{-1}): 1722 ($\nu_{C=O}$); 1643 ($\nu_{C=N}$); 1584; 1548; 1460; 1368. Anal. Calcd for $C_{22}H_{28}N_2O_2$: C, 74.97; H, 8.01; N, 7.95. Found: C, 74.71; H, 7.99; N, 7.69.

Ethyl 6-[1-((2,6-Difluorophenyl)imino)ethyl]pyridine-2-carboxylate (2d). A solution of 2,6-difluoroaniline (0.575 g, 4.34 mmol), ethyl 6-acetylpyridine-2-carboxylate (0.700 g, 3.62 mmol), *p*-toluenesulfonic acid (0.060 g), and silica−alumina catalyst (grade 135, 0.120 g) in toluene (25 mL) was refluxed for 15 h, and 4 Å molecular sieves (2 g) were added to remove water. After filtration and solvent evaporation, the crude product was purified by column chromatography on silica gel with petroleum ether/ethyl acetate (6/1) as eluent to afford the product as a viscous yellow oil in 44.5% yield. ^{1}H NMR (300 MHz, $CDCl_3$; δ): 8.52 (d, 1H, J = 7.8 Hz, Py H_m); 8.21 (d, 1H, J = 7.5 Hz, Py H_m); 7.94 (t, 1H, J = 7.8 Hz, Py H_p); 6.9−7.1 (m, 3H, Ar *H*); 4.49 (q, 2H); 2.47 (s, 3H); 1.46 (t, 3H). ^{13}C NMR (75.45 MHz, $CDCl_3$; δ): 172.47; 165.06; 155.98; 147.51; 145.49; 137.58; 128.25; 126.70; 125.07; 124.53; 124.45; 61.98; 17.60; 14.31. IR (KBr; cm^{-1}): 1721 ($\nu_{C=O}$); 1647 ($\nu_{C=N}$); 1583; 1471; 1425; 1369. Anal. Calcd for $C_{16}H_{14}F_2N_2O_2$: C, 63.15; H, 4.64; N, 9.21. Found: C, 63.06; H, 4.52; N, 9.10.

Table 5. Crystallographic Data and Refinement Details for 2b,c, 3b,c, 3e·CH_2Cl_2, 3f·CH_2Cl_2, 4c, and 4f·CH_2Cl_2

	2b	**2c**	**3b**	**3c**
formula	$C_{20}H_{24}N_2O_2$	$C_{22}H_{28}N_2O_2$	$C_{20}H_{24}Cl_2F\ N_2O_2$	$C_{22}H_{28}Cl_2F\ N_2O_2$
fw	324.41	352.46	451.16	479.21
cryst syst	monoclinic	triclinic	monoclinic	monoclinic
space group	$P2_1/c$	$P\bar{1}$	$P2_1/c$	$P2_1/n$
a (Å)	10.881(2)	8.566(3)	18.572(4)	9.8641(2)
b (Å)	21.536(4)	11.233(3)	8.1783(16)	18.0236(4)
c (Å)	7.9300(16)	22.545(7)	14.677(3)	13.0853(3)
α (deg)	90	103.851(5)	90	90
β (deg)	90.73(3)	91.796(6)	107.50(3)	93.224(3)
γ (deg)	90	93.920(6)	90	90
V (Å^3)	1853.8(6)	2098.8(11)	2126.1(7)	2322.71(9)
Z	4	4	4	4
D_{calcd} (g cm^{-3})	1.162	1.115	1.409	1.370
abs coeff, μ (mm^{-1})	0.075	0.071	0.977	0.899
F(000)	696	760	936	1000
θ range (deg)	2.66−26.39	0.93−25.00	1.15−27.48	2.26−27.75
no. of data collected	10 204	10 951	4840	5129
no. of unique data	3778	7382	4840	2064
R	0.0661	0.0624	0.0339	0.0414
R_w	0.1803	0.1371	0.0926	0.0513
goodness of fit	1.005	1.006	1.024	0.691

	3e·CH_2Cl_2	**3f**·CH_2Cl_2	**4c**	**4f**·CH_2Cl_2
formula	$C_{17}H_{16}Cl_6FeN_2O_2$	$C_{17}H_{16}Br_2Cl_4FeN_2O_2$	$C_{22}H_{28}Cl_2CoN_2O_2$	$C_{17}H_{16}Br_2Cl_4CoN_2O_2$
fw	548.87	637.79	482.29	640.87
cryst syst	triclinic	monoclinic	monoclinic	triclinic
space group	$P\bar{1}$	$P2_1/n$	$P2_1/n$	$P\bar{1}$
a (Å)	8.1888(16)	8.1968(16)	9.840(2)	8.1368(16)
b (Å)	8.9943(18)	8.9615(18)	17.844(4)	8.9650(18)
c (Å)	16.108(3)	16.470(3)	13.178(3)	16.349(3)
α (deg)	100.49(3)	102.26(3)	90	102.23(3)
β (deg)	98.71(3)	98.51(3)	92.85(3)	98.36(3)
γ (deg)	94.71(3)	94.46(3)	90	94.28(3)
V (Å^3)	1145.8(4)	1161.7(4)	2311.1(8)	1146.2(4)
Z	2	2	4	2
D_{calcd} (g cm^{-3})	1.591	1.823	1.386	1.857
abs coeff, μ (mm^{-1})	1.373	4.564	0.994	4.717
F(000)	552	624	1004	626
θ range (deg)	1.30−27.48	1.28−27.45	2.37−27.48	1.29−27.33
no. of data collected	5212	5245	4725	5012
no. of unique data	5212	5245	1929	5012
R	0.0459	0.0436	0.0432	0.0519
R_w	0.1288	0.1042	0.0538	0.1374
goodness of fit	1.039	1.021	0.708	1.045

Ethyl 6-[1-((2,6-Dichlorophenyl)imino)ethyl]pyridine-2-carboxylate (2e). Using a procedure analogous to that used for the synthesis of **2d**, **2e** was obtained as a viscous yellow oil in 34.4% yield. ^{1}H NMR (300 MHz, $CDCl_3$; δ): 8.58 (d, 1H, J = 7.8 Hz, Py H_m); 8.23 (d, 1H, J = 7.8 Hz, Py H_m); 7.96 (t, 1H, J = 7.8 Hz, Py H_p); 7.57 (d, 2H, J_1 = 8.1 Hz, Ar H); 7.00 (t, 1H, J = 8.0 Hz, Ar H); 4.50 (q, 2H); 2.38 (s, 3H); 1.46 (t, 3H). ^{13}C NMR (75.45 MHz, $CDCl_3$; δ): 171.19; 165.06; 155.62; 147.509; 145.490; 137.58; 128.25; 126.70; 125.07; 124.53; 124.45; 61.98; 17.60; 14.31. IR (KBr; cm^{-1}): 1721 ($\nu_{C=O}$); 1655 ($\nu_{C=N}$); 1580; 1556; 1437; 1368. Anal. Calcd for $C_{16}H_{14}Cl_2N_2O_2$: C, 56.99; H, 4.18; N, 8.31. Found: C, 56.84; H, 4.40; N, 7.99.

Ethyl 6-[1-((2,6-Dibromophenyl)imino)ethyl]pyridine-2-carboxylate (2f). Using a procedure analogous to that used for the synthesis of **2d**, **2f** was obtained as a viscous yellow oil in 63.8% yield. ^{1}H NMR (300 MHz, $CDCl_3$; δ): 8.59 (d, 1H, J = 7.8 Hz, Py H_m); 8.23 (d, 1H, J = 6.9 Hz, Py H_m); 7.97 (t, 1H, J = 7.8 Hz, Py H_p); 7.57 (q, 2H, J_1 = 7.5 Hz, J_2 = 0.6 Hz, Ar H); 6.88 (t, 1H, J = 7.8 Hz, Ar H); 4.49 (m, 2H); 2.37 (s, 3H); 1.46 (t, 3H). ^{13}C NMR (75.45 MHz, $CDCl_3$; δ): 170.89; 164.98; 155.49; 147.87; 147.48; 135.51; 131.93; 126.67; 125.36; 125.01; 113.40; 61.90; 17.55; 14.24. IR (KBr; cm^{-1}): 1720 ($\nu_{C=O}$); 1654 ($\nu_{C=N}$); 1582; 1548; 1430; 1368. Anal. Calcd for $C_{16}H_{14}Br_2N_2O_2$: C, 45.10; H, 3.31; N, 6.57. Found: C, 45.12; H, 3.37; N, 6.34.

Synthesis of (L)$FeCl_2$ (3a−f; L = 2a−f). The complexes **3a**−**f** were synthesized by the reaction of $FeCl_2$ with the corresponding ligands in ethanol. A typical synthetic procedure for **3a** can be described as follows. The ligand **2a** (0.100 g, 0.338 mmol) and $FeCl_2$ (0.043 g, 0.338 mmol) were added to a Schlenk tube, followed by the addition of freshly distilled ethanol (4 mL) with rapid stirring at room temperature. The solution turned deep blue immediately. The reaction mixture was stirred for 10 h, and absolute diethyl ether (10 mL) was added to precipitate the complex. After the mixture stood for 30 min, the supernatant was removed. The precipitate was washed with diethyl ether twice and dried in vacuo to furnish the pure product as a blue powder in 82.0% yield. Anal. Calcd for $C_{18}H_{20}Cl_2FeN_2O_2$: C, 51.10; H, 4.76; N, 6.62. Found: C, 50.43; H, 4.84; N, 6.15. IR (KBr; cm^{-1}): 1708 ($\nu_{C=O}$); 1624 ($\nu_{C=N}$); 1590; 1468; 1374 cm^{-1}. Data for **3b** are as follows. Yield: 80.0%. IR (KBr; cm^{-1}): 1699 ($\nu_{C=O}$); 1623 ($\nu_{C=N}$); 1588; 1448; 1376. Anal. Calcd for $C_{20}H_{24}Cl_2FeN_2O_2$: C, 53.24; H, 5.36; N, 6.21. Found: C, 52.71; H, 5.33; N, 6.09. Data for **3c** are as follows. Yield: 83.0%. IR (KBr; cm^{-1}): 1719 ($\nu_{C=O}$); 1619 ($\nu_{C=N}$); 1590; 1464; 1371. Anal. Calcd for $C_{22}H_{28}Cl_2FeN_2O_2$: C, 55.14; H, 5.89; N, 5.85. Found: C, 54.82; H, 5.86; N, 5.61. Data for **3d** are as follows. Yield: 80.0%. IR (KBr; cm^{-1}): 1711 ($\nu_{C=O}$); 1620 ($\nu_{C=N}$); 1591; 1472; 1375. Anal. Calcd for $C_{16}H_{14}Cl_2F_2FeN_2O_2$: C, 44.58; H, 3.27; N, 6.50. Found: C, 45.06; H, 3.44; N, 6.36. Data for **3e** are as follows. Yield: 81.0%. IR (KBr; cm^{-1}): 1701 ($\nu_{C=O}$); 1624 ($\nu_{C=N}$); 1589; 1564; 1436. Anal. Calcd for $C_{16}H_{14}Cl_4FeN_2O_2$: C, 41.42; H, 3.04; N, 6.04. Found: C, 41.32; H, 3.06; N, 5.99. Data for **3f** are as follows. Yield: 80.3%. IR (KBr; cm^{-1}): 1704 ($\nu_{C=O}$); 1625 ($\nu_{C=N}$); 1590; 1553; 1429. Anal. Calcd for $C_{16}H_{14}Br_2Cl_2FeN_2O_2$: C, 34.76; H, 2.55; N, 5.07. Found: C, 35.07; H, 2.57; N, 4.96.

Synthesis of (L)$CoCl_2$ (4a−f; L = 2a−f). **4a−f** were prepared by the same synthetic procedure as for **3a−f** and obtained as a green powder. The synthetic procedure of **4a** can be described as follows: to a mixture of ligand **2a** (0.150 g, 0.506 mmol) and $CoCl_2$ (0.065 g, 0.500 mmol) was added freshly distilled ethanol (8 mL) at room temperature. The solution turned green immediately. The reaction mixture was stirred for 5 h, and hexane (20 mL) was added to precipitate the complex. The precipitate was collected by filtration and washed with hexane, followed by drying in vacuo. The desired complex was obtained as a green powder in 68.0% yield. IR (KBr; cm^{-1}): 1713 ($\nu_{C=O}$); 1625 ($\nu_{C=N}$); 1591; 1468; 1374. Anal. Calcd for $C_{18}H_{20}Cl_2CoN_2O_2$: C, 50.73; H, 4.73; N, 6.57. Found: C, 50.65; H, 4.81; N, 6.39. Data for **4b** are as follows. Yield: 69.2%. IR (KBr; cm^{-1}): 1701 ($\nu_{C=O}$); 1624 ($\nu_{C=N}$); 1589; 1467; 1375. Anal. Calcd for $C_{20}H_{24}Cl_2CoN_2O_2$: C, 52.88; H, 5.33; N, 6.17. Found: C, 52.40; H, 5.33; N, 6.04. Data for **4c** are as follows. Yield: 72.0%. IR (KBr; cm^{-1}): 1722 ($\nu_{C=O}$); 1620 ($\nu_{C=N}$); 1591; 1464; 1371. Anal. Calcd for $C_{22}H_{28}Cl_2CoN_2O_2$: C, 54.79; H, 5.85; N, 5.81. Found: C, 54.73; H, 5.94; N, 5.45. Data for **4d** are as follows. Yield: 63.3%. IR (KBr; cm^{-1}): 1696 ($\nu_{C=O}$); 1630 ($\nu_{C=N}$); 1592; 1471; 1378. Anal. Calcd for $C_{16}H_{14}Cl_2CoF_2N_2O_2$: C, 44.27; H, 3.25; N, 6.45. Found: C, 44.22; H, 3.29; N, 6.19. Data for **4e** are as follows. Yield: 63.0%. IR (KBr; cm^{-1}): 1708 ($\nu\nu_{C=O}$); 1631 ($\nu_{C=N}$); 1590; 1563; 1436. Anal. Calcd for $C_{16}H_{14}Cl_4CoN_2O_2$: C, 41.15; H, 3.02; N, 6.00. Found: C, 41.17; H, 3.06; N, 5.61. Data for **4f** are as follows. Yield: 73.4%. IR (KBr; cm^{-1}): 1710 ($\nu_{C=O}$); 1626 ($\nu_{C=N}$); 1591; 1553; 1430. Anal. Calcd for $C_{16}H_{14}Br_2Cl_2CoN_2O_2$: C, 34.57; H, 2.54; N, 5.04. Found: C, 34.33; H, 2.57; N, 4.82.

Procedure for Oligomerizations and Polymerizations with 1 atm of Ethylene. The complex (5 μmol) was added to a Schlenk-type flask under nitrogen. The flask was back-filled three times with N_2 and twice with ethylene and then charged with toluene and MAO solution in turn under an ethylene atmosphere. In the cases that CH_2Cl_2 was used as the solvent, MAO was added first to the dry flask under a nitrogen atmosphere, and then toluene in the MAO solution was completely removed in vacuo, followed by addition of complex and CH_2Cl_2. At the prescribed temperature, the reaction solution was vigorously stirred under 1 atm of ethylene for the desired period of time. The polymerization reaction was quenched by addition of 60 mL of 10% HCl solution. About 1 mL of organic solution was dried with anhydrous Na_2SO_4 for GC determination. The remaining mixture was poured into 100 mL of ethanol to precipitate the polymer. The polyethylene was isolated via filtration and dried at 60 °C to constant weight in a vacuum oven.

Procedure for Oligomerization and Polymerizations with 10 atm of Ethylene. High-pressure ethylene polymerization was performed in a stainless steel autoclave (2 L capacity) equipped with a gas ballast through a solenoid clave for continuous feeding of ethylene at constant pressure. A 700 mL amount of toluene containing the catalyst precursor was transferred to the fully dried reactor under a nitrogen atmosphere. The required amount of cocatalyst (MAO) was then injected into the reactor using a syringe. As the prescribed temperature was reached, the reactor was pressurized to 10 atm. After the reaction mixture was stirred for the desired period of time, the reaction was quenched and the mixture worked up using the same method as described above for the 1 atm reaction.

X-ray Crystallographic Studies. Single-crystal X-ray diffraction studies for ligands **2b**,**c** were carried out on a Bruker SMART 1000 CCD diffractometer with graphite-monochromated Mo Kα radiation (λ = 0.710 73 Å). Intensity data for crystals of **3b**,**c**,**e**,**f** and **4c**,**f** were collected on a Rigaku RAXIS Rapid IP diffractometer with graphite-monochromated Mo Kα radiation (λ = 0.710 73 Å). Cell parameters were obtained by global refinement of the positions of all collected reflections. Intensities were corrected for Lorentz and polarization effects and empirical absorption. The structures were solved by direct methods and refined by full-matrix least squares on F^2. All non-hydrogen atoms were refined anisotropically. All hydrogen atoms were placed in calculated positions. Structure solution and refinement were performed by using the SHELXL-97 package. Crystal data and processing parameters for ligands **2b**,**c** and complexes **3b**,**c**,**e**,**f** and **4c**,**f** are summarized in Table 5.

Acknowledgment. We are grateful to the National Natural Science Foundation of China for financial support under Grant No. 20272062 and National 863 Project (Grant No. 2002AA333060). We thank Dr. Jinkui Niu for the English proofreading.

Supporting Information Available: Crystallographic data for **2b**,**c**, **3b**,**c**,**e**,**f**, and **4c**,**f** as CIF files. This material is available free of charge via the Internet at http://pubs.acs.org.

OM0496636